

Immunolectron microscopic analysis of dipeptidyl-peptidases and dipeptide transporter involved in nutrient acquisition in *Porphyromonas gingivalis*

Yu Shimoyama¹, Daisuke Sasaki^{2*}, Yuko Ohara-Nemoto^{1,3}, Takayuki K. Nemoto^{1,3}, Manami Nakasato², Minoru Sasaki¹, and Taichi Ishikawa¹

¹Division of Molecular Microbiology, Department of Microbiology, Iwate Medical University, 1-1-1 Idai-dori, Yahaba-Cho, Shiwa-Gun, Iwate, 028-3694, Japan

²Division of Periodontology, Department of Conservative Dentistry, Iwate Medical University School of Dentistry, 1-3-27 Chuo-dori, Morioka, Iwate, 020-8505, Japan

³Department of Pediatric Dentistry, Course of Medical and Dental Sciences, Nagasaki University Graduate School of Biomedical Sciences, Sakamoto 1-7-1, Nagasaki 852-8588, Japan

*Corresponding author: Daisuke Sasaki, Division of Periodontology, Department of Conservative Dentistry, Iwate Medical University School of Dentistry, 1-3-27 chuo-dori, Morioka, Iwate 020-8505, Japan,

Tel: +81-19-651-5111; E-mail: daisukes@iwate-med.ac.jp

ORCID ID

Yu Shimoyama : 0000-0002-4143-6519

Daisuke Sasaki : 0000-0002-8260-0717

Yuko Ohara-Nemoto : 0000-0002-2822-7296

Takayuki K. Nemoto : 0000-0002-5007-6260

Manami Nakasato : No ID

Minoru Sasaki : 0000-0002-6105-2424

Taichi Ishikawa : 0000-0002-6229-0379

Abstract

Porphyromonas gingivalis is an asaccharolytic, Gram-negative, anaerobic bacterium representing a keystone pathogen in chronic periodontitis. The bacterium's energy production depends on the metabolism of amino acids, which are predominantly incorporated as dipeptides via the proton-dependent oligopeptide transporter (Pot). In this study, the localization of dipeptidyl-peptidases (DPPs) and Pot was investigated for the first time in *P. gingivalis* using immunoelectron microscopy with specific antibodies for the bacterial molecules and gold-conjugated secondary antibodies on ultrathin sections. High-temperature protein G and hemin-binding protein 35 were used as controls, and the cytoplasmic localization of the former and outer membrane localization of the latter were confirmed. *P. gingivalis* DPP4, DPP5, DPP7, and DPP11, which are considered sufficient for complete dipeptide production, were detected in the periplasmic space. In contrast, DPP3 was localized in the cytoplasmic space in accord with the absence of a signal sequence. The inner membrane localization of Pot was confirmed. Thus, spatial integration of the nutrient acquisition system exists in *P. gingivalis*, in which where dipeptides are produced in the periplasmic space by DPPs and readily transported across the inner membrane via Pot.

Keywords: Dipeptidyl-peptidase, Immunoelectron microscopy, Periplasmic space, Peptidoglycan layer, *Porphyromonas gingivalis*, Proton-dependent oligopeptide transporter

Introduction

Porphyromonas gingivalis, a Gram-negative anaerobe, is closely associated with chronic periodontitis [1] and has been further linked to systemic diseases, including type 2 diabetes mellitus, cardiovascular diseases, rheumatoid arthritis, and Alzheimer's disease [2-5].

P. gingivalis can not metabolize carbohydrates, and its growth depends on amino acid metabolism [6]. Nutritional extracellular proteins are initially degraded to oligopeptides by endopeptidases, *i.e.*, arginine- and lysine-specific gingipains [7], before being transferred through the outer membrane into the periplasmic space. RagAB has recently been identified as a molecule involved in the uptake of oligopeptides [8]. Dipeptidyl-peptidases (DPPs) then cleave oligopeptides to form dipeptides [9]. Concerning amino acid incorporation, three amino acids/oligopeptide transporters have been identified in *P. gingivalis*. These are the serine/threonine transporter (SstT) (PGN_1640), proton-dependent oligopeptide transporter (Pot) (PGN_0135), and oligopeptide transporter (Opt) (PGN_1518)[10,11]; Pot has been identified as the transporter responsible for dipeptide incorporation [11].

P. gingivalis possesses five dipeptidyl-peptidase genes consisting of DPP3 (PGN_1645), DPP4 (PGN_1469), DPP5 (PGN_0756), DPP7 (PGN_1479), and DPP11 (PGN_0607), which convert oligopeptides into dipeptides[12-15]. Because the substrate specificity of DPPs varies primarily at the penultimate position from the N-terminus (P1 position), combining these peptidases can ensure complete conversion of oligopeptides to dipeptides [16, 17]. Two exopeptidases, acylpeptidyl-oligopeptidase (AOP) (PGN_1349)[18] and prolyl tripeptidyl-peptidase A (PTP-A) (PGN_1149) [19], aid in dipeptide production because the former is highly preferential to N-terminally acylated peptides and the latter is specific for peptides with Pro at the third position from the N-terminus as DPPs do not metabolize types of these peptides.

The discussion above postulated that DPPs are localized between the inner and outer membranes. Accordingly, the subcellular fractionation of *P. gingivalis* previously demonstrated DPP5 localization in the periplasmic space (15). To our knowledge, immunoelectron microscopy (IEM) for soluble proteins on *P. gingivalis* ultrathin sections has not been reported to date. In this study, we used this method for the first time to investigate the localization of proteins involved in nutrient acquisition in the bacterium.

Materials and Methods

Antibodies

Polyclonal antiserum against recombinant DPP3, DPP4, DPP5, DPP11 [14,15,20], DPP7 [21], and High-temperature protein G (HtpG) [22] of *P. gingivalis* were previously described. Anti-Pot peptide (C-M¹³⁴YDNDTYRDKR¹⁴⁴-OH) rat Ig was prepared by Scrum (Tokyo, Japan). Dr. Mikio Shoji (Nagasaki University) kindly provided the antihemoglobin-binding protein 35 (HBP35) (PGN_0659) rabbit serum.

Preparation of resin-embedded bacteria for IEM

P. gingivalis ATCC 33277 was cultured in anaerobic bacteria culture media (Eiken Chemical, Tokyo, Japan) supplemented with 5- $\mu\text{g mL}^{-1}$ hemin (Fujifilm Wako Pure Chemical, Osaka, Japan) and 0.5- $\mu\text{g mL}^{-1}$ menadione (Sigma-Aldrich, St. Louis, MO, U.S.A) at 37°C for 48 h under anaerobic conditions [14]. Bacteria (1×10^8 cells) were rinsed with PBS (-) (Nacalai Tesque, Kyoto, Japan) and fixed with 4% paraformaldehyde (Fujifilm Wako Pure Chemical) at room temperature for 4 h and then washed twice with 0.1-M PBS (-) and dehydrated with a graded series of ethanol (70% \rightarrow 80% \rightarrow 90% \rightarrow 100% $\times 2$). Samples were immersed in 50% (v/v) acetonitrile in ethanol at 4°C for 1 h and infiltrated with LR White resin (London Resin Company Ltd., London, UK) overnight at 4°C. Then, samples were polymerized at 60°C for 24 h. The resin-embedded samples were sliced into 50–80 nm ultrathin sections and collected on nickel grids (Nisshin EM, Tokyo, Japan) [23].

Immunoelectron microscopy (IEM)

IEM was performed as previously reported [24]. Briefly, nickel grids were blocked with 10% goat serum (Abcam, Cambridge, UK) in 0.1-M TBS at room temperature for 2 h. After washing with 0.1-M TBS, nickel grids were incubated at 4°C with anti-*P. gingivalis* HtpG, HBP35, Pot, DPP3, DPP4, DPP5, DPP7, or DPP11 antibody (dilution, 1:5, 1:50, 1:1, 1:100, 1:50, 1:200, 1:200, or 1:50, respectively). After 48 h, the nickel grids were washed with 0.1-M TBS and incubated with 1:100 dilution of 10-nm gold-conjugated goat antirat IgG for anti-Pot Ig, or antirabbit IgG (Abcam) for others at room temperature for 2 h. Then, samples were washed four times with 0.1-M TBS and four times with MQ water. All samples were

air-dried and observed under a Hitachi H-7650 electron microscope (Hitachi High-Tech Co., Tokyo, Japan). The antiserum and second Ig dilution rates were determined to minimize nonspecific background. Each image was captured at 10 000× and 25 000× magnifications. The number of colloidal golds was counted in three observations.

Results and Discussion

IEM of *P. gingivalis* proteins

Initially, HtpG and HBP35 were used as references for immunological detection. HtpG is a human Hsp90 homolog of bacteria localized in the cytoplasm [25], and HBP35 is an outer membrane protein with a conserved C-terminal domain [26]. As depicted in Fig. 1A, HtpG was solely observed in the cytoplasm. Most dots for HBP35 were observed near the edge of the cell surface, corresponding to the outer membrane (Fig. 1B, blue arrow). The periplasmic space surrounding the cytoplasm was depicted as an intermediate dense layer, with the middle line representing the peptidoglycan layer. The thickness of the periplasmic space was calculated as 23.7 ± 1.5 nm ($n = 9$). The inner membrane corresponded to the border between the cytoplasm and periplasmic space. The outer membrane was ambiguous, possibly because of its thin structure and presence of circumferential fimbriae.

Next, we examined the localization of Pot. *P. gingivalis* Pot contains 12 transmembrane α -helix motifs, which may be anchored in the inner membrane[11], and the antibody was raised against a deduced cytoplasmic region (M¹³⁴YDNDTYRDKR¹⁴⁴) between transmembrane helices 4 and 5. Pot was localized at the border region between the cytoplasm and periplasmic space, i.e. the inner membrane (Fig. 1C).

DPP localization

We then examined the localization of DPPs by IEM. DPP3 was exclusively located in the cytoplasm (Fig. 2A). In contrast, DPP4 and DPP5 tended to be localized in the periplasmic space (Fig. 2B and C), which is consistent with our previous research on the localization of DPP5 by cell fractionation and western blotting [15]. DPP7 and DPP11 were detected in greater abundance in the periplasmic space than DPP4 and DPP5 (Fig. 2D and E). More than half of these four DPPs appeared attached to the peptidoglycan layer (Fig. 2, red arrow).

Table 1 summarizes the localization of the proteins examined by IEM images. Several dots of the four DPPs were detected in the cytoplasm and inner membrane, which might represent newly synthesized molecules and molecules passing through the inner membrane, respectively. Most dots of the four DPPs in the periplasmic space appeared to be associated with the peptidoglycan layer. Because DPP11 has a molecular size of 12.8 Å in a substrate-bound state and 16.6 Å in an unbound state [27], and the smallest pore of the peptidoglycan layer is estimated to be 70 Å across [28], DPPs seem to freely pass through peptidoglycan pores. Nevertheless, it should be noted that current IEM observations indicate a specific interaction of DPPs with the peptidoglycan layer. Whether there is an interaction between DPPs and peptidoglycan should be carefully examined in future studies. In a recent proteome analysis, periplasmic localization of DPP4, DPP5, DPP7, and DPP11 has been also proposed [29].

DPP4, DPP5, DPP7, and DPP11, as well as AOP and PTP-A, possess typical N-terminal signal sequences [11], and the N-terminal 21-residue signal sequence of DPP11 was processed in *Porphyromonas endodontalis* [14]. Therefore, these molecules should be processed and secreted from the inner membrane. In contrast, DPP3 found in the cytoplasm lacks the sequence and could be involved in the degradation of endogenous proteins.

Conclusion

This IEM study demonstrated the periplasmic localization of DPP4, DPP5, DPP7, and DPP11 and the existence of the dipeptide transporter Pot on the inner membrane in *P. gingivalis*. These results indicate an effective integration of the bacterial nutrient acquisition system composed of DPPs for dipeptide production and Pot for uptake.

Acknowledgements

We thank Dr. Mikio Shoji (Nagasaki University) for kindly providing the anti-HBP35 antibody and Mr. Ishida, Mr. Hanasaka, and Mrs. Ishiyama at the Technical Support Center for Life Science Research of Iwate Medical University for their kind assistance of the TEM observation.

Declarations

Funding

This work was supported by JSPS KAKENHI Grant [grant number JP18K09557 to Y.S., JP19K10045 to T.K.N., JP19K10071 to Y.O.N., and JP19K19005 to M.N.].

Conflicts of interest

The authors declare that they have no conflicts of interest with the contents of this article.

Ethical approval

Not applicable

Consent to participate

Not applicable

Consent for publication

Not applicable

Availability of data and material

All data generated or analysed during this study are included in this published article.

Code availability

Not applicable

Authors contributions

Y.S., D.S., Y.O.-N. and T.K.N. conceptualization; Y.S., D.S., M.N., M.S., and T.I. methodology; T.K.N. resources; Y.S., D.S., Y.O.-N., T.K.N. and T.I. writing-review and editing; Y.O.-N. visualization; T.K.N, and M.S. supervision; Y.S., Y.O.-N., T.K.N. and M.N. funding acquisition.

References

1. Holts CS, Ebersole LJ (2005) *Porphyromonas gingivalis*, *Treponema denticola*, and *Tannerella forsythia*: the 'red complex', a prototype polybacterial pathogenic consortium in periodontitis. *Periodontology* 2000 38:72–122
2. Renvert S, Pettersson T, Ohlsson O, et al. (2006) Bacterial profile and burden of periodontal infection in subjects with a diagnosis of acute coronary syndrome. *J Periodontol* 77:1110–1119
3. Ohki T, Itabashi Y, Kohno T, et al. (2012) Detection of periodontal bacteria in thrombi of patients with acute myocardial infarction by polymerase chain reaction. *Am Heart J* 163:164–167
4. Arimatsu K, Yamada H, Miyazawa H, et al. (2014) Oral pathobiont induces systemic inflammation and metabolic changes associated with alteration of gut microbiota. *Sci Rep* 4:4828
5. Yamada C, Akkaoui J, Ho A, et al. (2020) Potential role of phosphoglycerol dihydroceramide produced by periodontal pathogen *Porphyromonas gingivalis* in the pathogenesis of Alzheimer's disease. *Front Immunol* 11:591571
6. Citron DM, Poxton IR, Baron EJ (2007) *Bacteroides*, *Porphyromonas*, *Prevotella*, *Fusobacterium*, and other anaerobic Gram-negative rods. In: Murray PR, Baron EJ, Jorgensen JH, et al. (eds) *Manual of clinical microbiology*, 9th edn. American Society for Microbiology, Washington, pp911–932
7. Potempa J, Sroka A, Imamura T, et al. (2003) Gingipains, the major cysteine proteinases and virulence factors of *Porphyromonas gingivalis*: structure, function and assembly of multidomain protein complexes. *Curr Protein Pept Sci* 4:397–407
8. Madej M, White JBR, Nowakowska Z, et al. (2020) Structural and functional insights into oligopeptide acquisition by the RagAB transporter from *Porphyromonas gingivalis*. *Nat Microbiol* 5:1016–1025
9. Nemoto TK, Ohara-Nemoto Y (2016) *Porphyromonas gingivalis* exopeptidases as crucial factors for its amino acid metabolism. *Jpn Dent Sci Rev* 52:22–29
10. Dashper SG, Brownfield L, Slakeski N, et al. (2001) Sodium ion-driven serine/threonine transport in *Porphyromonas gingivalis*. *J Bacteriol* 183:4142–4148
11. Ohara-Nemoto Y, Sarwar TM, Shimoyama Y, et al. (2020) Preferential dipeptide incorporation of *Porphyromonas gingivalis* mediated by proton-dependent oligopeptide transporter (Pot). *FEMS Microbiol Lett* 367:fnaa204

12. Banbula A, Bugno M, Goldstein J, et al. (2000) Emerging family of proline-specific peptidases of *Porphyromonas gingivalis*: purification and characterization of serine dipeptidyl peptidase, a structural and functional homologue of mammalian prolyl dipeptidyl peptidase IV. *Infect Immun* 68:1176–1182
13. Banbula A, Yen J, Oleksy A, et al. (2001) *Porphyromonas gingivalis* DPP-7 represents a novel type of dipeptidylpeptidase. *J Biol Chem* 276:6299–6305
14. Ohara-Nemoto Y, Shimoyama Y, Kimura S, et al. (2011) Asp- and Glu-specific novel dipeptidyl peptidase 11 of *Porphyromonas gingivalis* ensures utilization of proteinaceous energy sources. *J Biol Chem* 286:38115–38127
15. Ohara-Nemoto Y, Rouf SM, Naito M, et al. (2014) Identification and characterization of prokaryotic dipeptidyl-peptidase 5 from *Porphyromonas gingivalis*. *J Biol Chem* 289:5436–5448
16. Nemoto TK, Ohara-Nemoto Y (2021) Dipeptidyl-peptidases: Key enzymes producing entry forms of extracellular proteins in asaccharolytic periodontopathic bacterium *Porphyromonas gingivalis*. *Mol Oral Microbiol* 36:145–156
17. Ohara-Nemoto Y, Shimoyama Y, Ono T, et al. (2022) Expanded substrate specificity supported by P1' and P2' residues enables bacterial dipeptidyl-peptidase 7 to degrade bioactive peptides. *J Biol Chem* 298:101585
18. Nemoto TK, Ohara-Nemoto Y, Bezerra GA, et al. (2016) A *Porphyromonas gingivalis* periplasmic novel exopeptidase, acylpeptidyl oligopeptidase, releases N-acylated di- and tripeptides from oligopeptides. *J Biol Chem* 291:5913–5925
19. Banbula A, Mak P, Bugno M, et al. (1999) Prolyl tripeptidyl peptidase from *Porphyromonas gingivalis*. A novel enzyme with possible pathological implications for the development of periodontitis. *J Biol Chem* 274:9246–9252
20. Ohara-Nemoto, Y, Nakasato, M, Shimoyama, Y, et al. (2017) Degradation of incretins and modulation of blood glucose levels by periodontopathic bacterial dipeptidyl peptidase 4. *Infect Immun* 85:e00277-17
21. Nishimata H, Ohara-Nemoto Y, Baba TT, et al. (2014) Identification of dipeptidyl-peptidase (DPP)5 and DPP7 in *Porphyromonas endodontalis*, distinct from those in *Porphyromonas gingivalis*. *PLoS One* 9:e114221
22. Kawano T, Kobayakawa T, Fukuma Y, et al. (2004) A comprehensive study on the immunological reactivity of the Hsp90 molecular chaperone. *J Biochem* 136:711–722

23. Sasaki M, Shimoyama Y, Kodama Y, et al. (2021) Abiotrophia defective DnaK promotes fibronectin-mediated adherence to HUVECs and induces a proinflammatory response. *Int J Mol Sci* 22(16):8528.
24. Sasaki M, Kodama Y, Shimoyama Y, et al. (2020) Abiotrophia defectiva adhere to saliva-coated hydroxyapatite beads via interactions between salivary proline-rich-proteins and bacterial glyceraldehyde-3-phosphate dehydrogenase. *Microbiol Immunol* 64:719–729
25. Lopatin ED, Jaramillo E, Edwards AC, et al. (1999) Cellular localization of a Hsp90 homologue in *Porphyromonas gingivalis*. *FEMS Microbiol lett* 181:9–16
26. Shoji M, Sato K, Yukitake H, et al. (2011) Por secretion system-dependent secretion and glycosylation of *Porphyromonas gingivalis* hemin-binding protein 35. *PLoS ONE* 6:e21372
27. Sakamoto Y, Suzuki Y, Iizuka I, et al. (2015) Structural and mutational analyses of dipeptidyl peptidase 11 from *Porphyromonas gingivalis* reveal the molecular basis for strict substrate specificity. *Sci Rep* 5:11151
28. Meroueh SO, Bencze KZ, Heseck D, et al. (2006) Three-dimensional structure of the bacterial cell wall peptidoglycan. *Proc Natl Acad Sci USA* 103:4404–4409
29. Veith PD, Shoji M, Scott NE, et al. (2022) Characterization of the O-glycoproteome of *Porphyromonas gingivalis*. *Microbiol Spectr* 10:e0150221

Table 1. Localization of *P. gingivalis* proteins analyzed by IEM

Protein	CP	IM	PL	PS	OM	Total	Localization
	%						
Dot number (mean \pm S.D.)							
HtpG	81.3 (8.7 \pm 1.5)	6.5 (0.7 \pm 0.6)	6.5 (0.7 \pm 0.6)	0 (0.0 \pm 0.0)	6.5 (0.7 \pm 1.2)	100 (10.7 \pm 0.6)	CP
HBP35	16.3 (1.3 \pm 1.2)	8.8 (0.7 \pm 0.6)	16.3 (1.3 \pm 1.2)	12.5 (1.0 \pm 1.0)	46.3 (3.7 \pm 1.2)	100 (8.0 \pm 1.0)	OM
Pot	41.1 (3.7 \pm 1.2)	55.6 (5.0 \pm 1.7)	3.3 (0.3 \pm 0.6)	0 (0.0 \pm 0.0)	0 (0.0 \pm 1.2)	100 (9.0 \pm 1.2)	IM
DPP3	77.6 (8.7 \pm 1.5)	6.5 (0.7 \pm 0.6)	2.8 (0.3 \pm 0.6)	6.5 (0.7 \pm 0.6)	2.8 (0.3 \pm 0.6)	100 (10.7 \pm 0.6)	CP
DPP4	40.0 (8.0 \pm 3.6)	1.5 (0.3 \pm 0.6)	36.5 (7.3 \pm 2.9)	16.5 (3.3 \pm 3.2)	5.0 (1.0 \pm 1.7)	100 (20.0 \pm 1.7)	PL
DPP5	24.3 (9.3 \pm 4.9)	9.7 (3.7 \pm 1.2)	39.2 (15.0 \pm 4.4)	19.1 (7.3 \pm 2.5)	7.8 (3.0 \pm 2.0)	100 (38.3 \pm 2.90)	PL
DPP7	15.8 (3.0 \pm 2.0)	14.2 (2.7 \pm 1.5)	43.7 (8.3 \pm 2.1)	26.3 (5.0 \pm 2.7)	0 (0.0 \pm 0.0)	100 (19.0 \pm 3.5)	PL
DPP11	24.3 (4.3 \pm 2.9)	13.0 (2.3 \pm 2.5)	32.2 (5.7 \pm 1.5)	18.6 (3.3 \pm 1.2)	11.3 (2.0 \pm 1.0)	100 (17.7 \pm 1.5)	PL

CP, cytoplasm; IM, inner membrane; PL, dots adhered to the peptidoglycan layer; PS, dots located in the periplasmic space but not associated with the layer; OM, outer membrane.

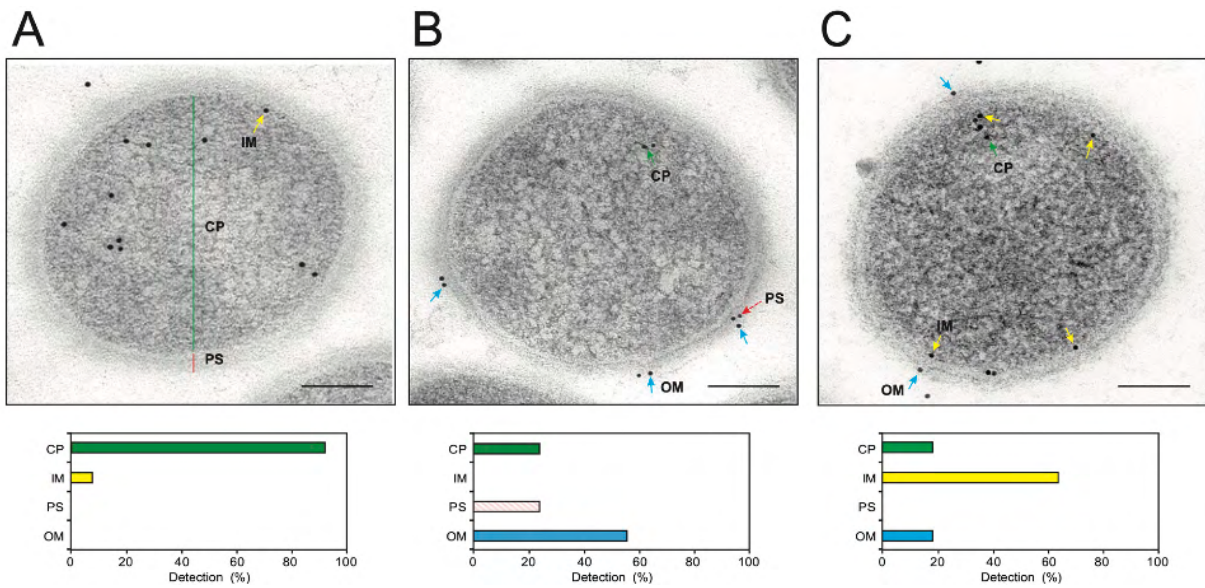


Fig. 1 Immunoelectron microscopic analysis on HtpG, HBP35, and Pot in *P. gingivalis*

Ultrathin sections were incubated with anti- (A) HtpG, (B) HBP35, or (C) Pot antiserum, followed by 10-nm gold-conjugated secondary IgG. Areas of the cytoplasm (CP) and periplasmic space (PS) are indicated in panel A. Dots localized in CP, on the outer membrane (OM), inner membrane (IM), and in PS are indicated by green, yellow, blue, and red arrows, respectively. The detection rates (%) of molecules are indicated at the bottom. Bars are 100 nm.

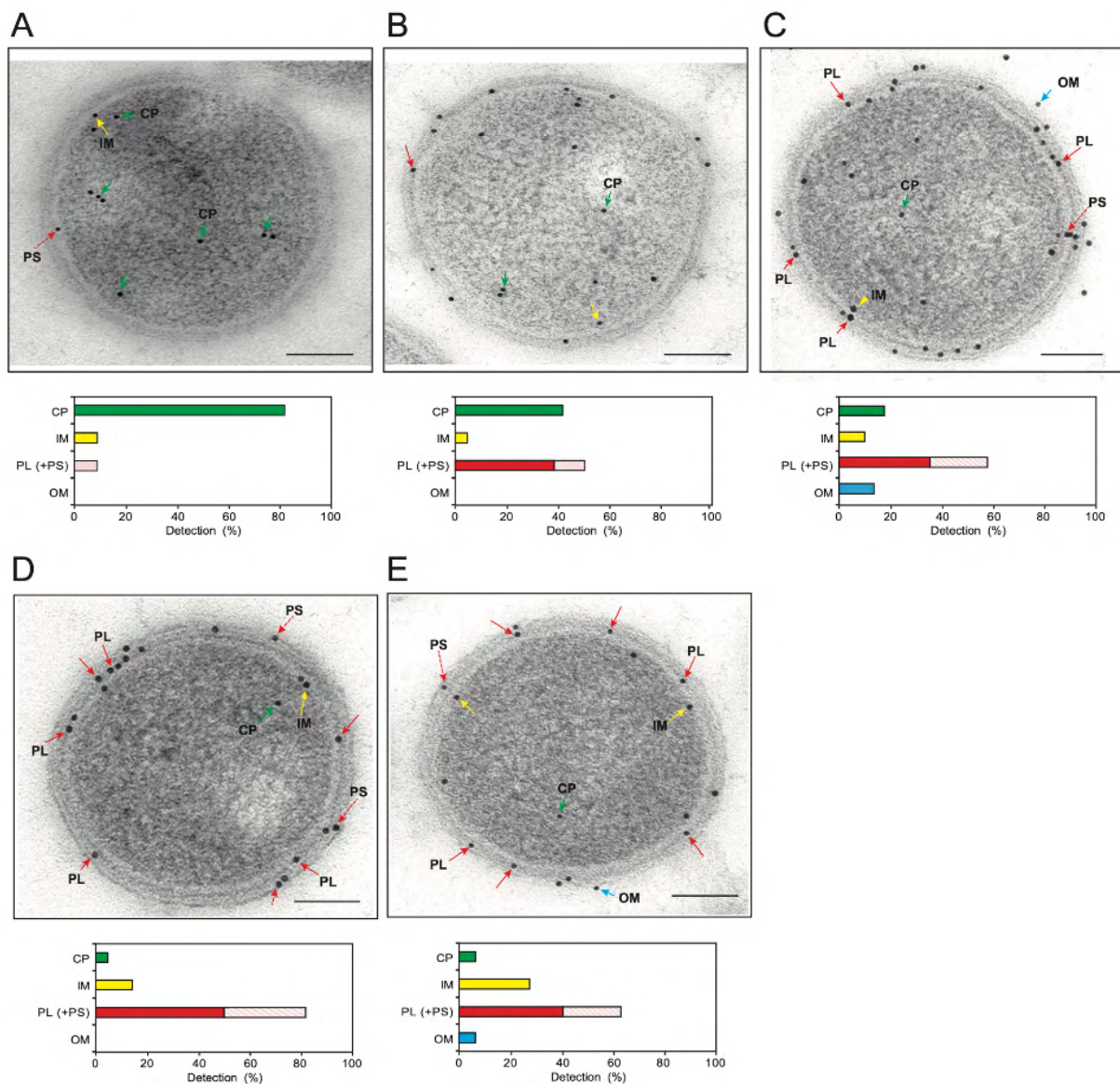


Fig. 2 Immunoelectron microscopy analysis on *P. gingivalis*

DPPs(A) DPP3, (B) DPP4, (C) DPP5, (D) DPP7, and (E) DPP11 were detected with each primary antibody and gold-conjugated antirabbit IgG. The detection rates (%) of molecules in the cytoplasm (CP), inner membrane (IM), peptidoglycan layer (PL), periplasmic space (PS), and outer membrane (OM) are indicated. Dots adhered to the peptidoglycan layer are indicated by red arrows, and those in the periplasmic space are shown by red broken arrows. Bars are 100 nm.